Hindawi
Shock and Vibration
Volume 2019, Article ID 9483246, 14 pages
https://doi.org/10.1155/2019/9483246

Research Article

Dynamic Amplification Factor of Shear Force on Bridge Columns under Impact Load

Haiying Ma,[1] **Zhen Cao**,[2] **Xuefei Shi**,[3] **and Junyong Zhou**[4]

[1]*Assistant Professor, Department of Bridge Engineering, Tongji University, Shanghai 200092, China*
[2]*Ph.D. Candidate, Department of Bridge Engineering, Tongji University, Shanghai 200092, China*
[3]*Professor, Department of Bridge Engineering, Tongji University, Shanghai 200092, China*
[4]*Lecturer, College of Civil Engineering, Guangzhou University, Guangzhou 510006, Guangdong, China*

Correspondence should be addressed to Xuefei Shi; shixf@tongji.edu.cn

Received 12 November 2018; Revised 18 January 2019; Accepted 12 February 2019; Published 10 March 2019

Academic Editor: Chengzhi Shi

Shear failure is a common mode for bridge column collapse during a vehicle-column collision. In current design codes, an equivalent static load value is usually employed to specify the shear capacity of bridge columns subject to vehicle collisions. But how to consider the dynamic effect on bridge columns induced by impact load needs further research. The dynamic amplification factor (DAF) is generally used in the analysis and design to include the dynamic effect, which is usually determined using the equivalent single degree of freedom (SDOF) method. However, SDOF method neglects the effect of the higher-order modes, leading to big difference between the calculated results and the real induced forces. Therefore, a novel method to obtain dynamic response under concentrated impact load including the effect of higher-order modes is proposed in the paper, which is based on the modified Timoshenko beam theory (MTB) and the classical Timoshenko beam theory (CTB). Finite element models are conducted to validate the proposed method. The result comparisons show that the results from the proposed method have more accuracy compared with the results from the CTB theory. Additionally, the proposed method is employed to calculate the maximum DAF of shear forces for bridge columns under impact load. Parametric studies are conducted to investigate the effect on the DAF of shear forces including slenderness ratio, boundary condition, and shape and position of impact load. Finally, a simplified formula for calculating the maximum DAF of shear force is proposed for bridge column design.

1. Introduction

Vehicle-column collisions occurred occasionally for bridge columns in recent years. Among them, bridge columns often collapsed with shear failure. For example, on April 17, 2009, a cement tanker truck crashed into two columns of an overpass at Jingzhu Expressway in Chenzhou, Hunan Province, China, and the accident led to shear failure at the top and bottom of the columns [1]. On September 8, 2006, a tractor-trailer hit the bridge column crossing IH-45 in Corsicana, Texas, United States, and it resulted in the failure of the column with two shear failure planes [2].

In structure design, shear failure should be avoided since it is a brittle failure and reduces the structural capacity to absorb energy [3]. The failure modes of reinforced concrete structures under impact loads are quite different from those under static loads. In a drop-weight test, for the reinforced concrete beams conducted by Saatci and Vecchio [4], the specimen subjected to shear failure under impact load even it was flexure-critical under static load. This is because the impact load excites high-order vibration modes resulting in internal force distribution different from the one under static load, which is the dynamic effect induced by the impact load [5].

The current specifications consider the impact load caused by vehicle collision to bridge columns, but there are still some deficiencies in the consideration of dynamic effects. The provisions in AASHTO-LRFD [6] specify that bridge columns shall be designed for an equivalent static force of 2670 kN (600 kips) with a distance of 1.50 m (5.0 ft) above ground, which is based on the research by Buth et al. [7]. In the full-scale test of vehicle collision of a bridge column conducted by Buth et al. [7], the column was

represented as a rigid cylinder resting upon a plate, the column was permitted to slide without friction, and the support system was simplified to two linear springs; therefore, the dynamic response within the column is not considered in AASHTO-LRFD.

In Annex C of Eurocode 1: Part 1–7, it is recommended that for hard impact from road traffic, actions due to impact should be determined by a dynamic analysis or represented by an equivalent static force [8]. When dynamic analysis is adopted, the force due to impact can be considered as a rectangular pulse, and the dynamic effect needs to be considered by dynamic amplification factor (DAF), where DAF means the ratio between dynamic and static response. The recommended values of DAF given in the Eurocode 1 are determined by Biggs research using single degree of freedom system (SDOF) [9]. The research by Biggs and Testa [9] obtained the DAFs of displacement of single degree of freedom system under different shape of loads, and it is assumed that the DAF of shear force is equal to the DAF of displacement when determining the dynamic shear force response using SDOF method. The effect of high-order modes on shear force is much bigger than that on displacement and bending moment. The accuracy of bending moment calculated by the SDOF method can meet the engineering requirement, but the error is large when calculating dynamic shear force [10]. Therefore, the DAF calculation in Eurocode 1 does not include the different dynamic effect to displacement, bending moment, and shear force.

Experimental study, finite element models, and analytic method can be used to obtain the dynamic response under impact load. The experiment is expensive, and the measurement accuracy is difficult to guarantee. The time-history of impact load was analyzed by Buth et al. [7], but the dynamic response of the structure was not obtained in the research. The drop-weight test was conducted by Saatci and Vecchio [4] to obtain the distribution of shear force and bending moment with measured acceleration distribution, but the accuracy was not high. Numerical method can obtain more accurate results, but it takes much more time for models and analysis process. The numerical simulation was conducted by El-Tawil et al. [11] to investigate the behavior of two bridge columns under vehicle collision, and the simulation only included the collision process of two types of vehicles.

Analytic method has higher computation efficiency among the above methods. The dynamic response of a simply supported beam at the early stage under blast load was studied by Magnusson et al. [12] using Bernoulli–Euler beam theory. The DAF of shear of a simply supported beam under impulsive load due to conventional weapon explosion was studied by Fang et al. [13] using Bernoulli–Euler beam theory and the CTB theory.

The research by Jones [14] showed that only the bending and transverse inertia were included in Bernoulli–Euler beam theory, and it overestimated the natural vibration frequency, which caused big error for dynamic shear force response. The CTB theory involves the shear deformation and rotational inertia caused by the bending deformation. When the CTB theory is used to solve the natural frequencies and modes, it is necessary to first determine a critical frequency independent on the beam length [15], and the obtained natural frequencies and modes may have errors [16]. The modified Timoshenko beam (MTB) motion equations including the rotational inertia caused by the shear deformation were proposed by Wan [16]. The higher-order natural frequencies obtained from the MTB theory are more practical than the CTB theory. However, the prerequisite for orthogonality is that the boundary conditions and loads are symmetric. For an impact load applied to bridge columns, it can be treated as concentrated load, which easily causes higher mode vibration compared with distributed impact load. The load position has a big effect on the response as well. Therefore, the analyses including unsymmetrical boundary condition and concentrated impact load are required for bridge column dynamic response analyses.

To accurately obtain the dynamic response of bridge columns under impact load, a novel method is proposed based on both the CTB and MTB theories in the paper. The proposed method is validated with finite element model analyses and compared with the results using the CTB theory. The maximum DAF of shear force under different conditions are obtained; parametric study is developed including slenderness ratio, boundary condition, characteristics, and position of impact load. Load characteristics include the load shape and growth time, and different load characteristics cause different dynamic response of bridge columns, which can affect the failure modes. Finally, three simplified formulas for calculating DAF of dynamic shear force are proposed to simplify the calculation including the dynamic effect for bridge columns under impact load.

2. Improved Calculation Method of Bridge Column Dynamic Response under Impact Load

2.1. Column Model. The research by Williamson [3] showed that the boundary conditions of bridge columns could be treated as fixed at the bottom (e.g., one end) and fixed or hinged at the top (e.g., the other end) based on the investigation of design and construction requirements of DOTs in the different states in the United States. In this paper, two boundary conditions including fixed both at bottom and at the top (i.e., F-F) and fixed at bottom and hinged at the top (i.e., F-H) are considered as shown in Figure 1. The height of the column is denoted by L. The coordinate system is built taking the fixed end as the origin. y-Axis is the lateral displacement direction of the bridge column, and x-axis is the direction along the column height. The impact force, P, is horizontally loaded on the column with a distance of ξL from the column end. In the figure, h is the cross section depth of the column; A is the cross section area of the column; I is the moment of inertia of the column cross section about the neutral axis; ρ is the density of the material; E is the elastic modulus; and G is the shear modulus.

r_g is the radius of rotation of the column cross section, which is equal to $\sqrt{(I/A)}$. The slenderness ratio is denoted as s, which is equal to u_{1L/r_g}, where u_1 is the coefficient of the column length, taken as 0.5 and 0.7 for F-F and F-H

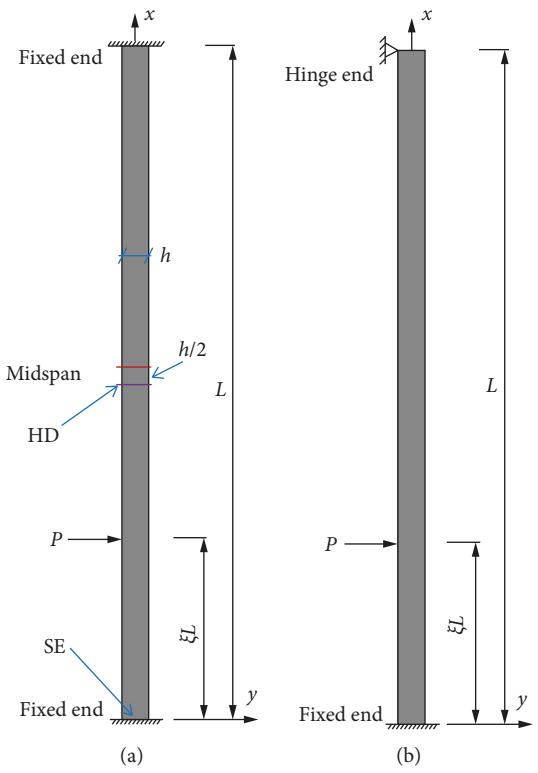

FIGURE 1: Different boundary conditions for the bridge columns. (a) F-F. (b) F-H.

boundary conditions, respectively. Obviously, the slenderness ratio for F-H condition is 1.4 times larger than that for F-F condition for the same column. Note that the slenderness ratios considered in the paper refers to that along the direction of the impact load.

2.2. Shape of Impact Load. The equation of impact load is formulated as

$$P = P_0 \cdot f(t), \tag{1}$$

where P_0 is the peak value of impact load and $f(t)$ is a function that represents the changing regulation of impact load along with time of t. The duration of impact load is denoted as t_d. For vehicle impact, the load characteristics change along with vehicle mass and impact velocity [17]. According to the shape of $f(t)$, a pulse load has different shapes, and the corresponding structural responses are different.

The right triangular load pulse without growth time is used to represent an impact load induced by rigid body. When the rigid part of vehicle (e.g., engine) impacts bridge columns, the load can be treated as a right triangle shape without growth time. When other parts of a vehicle impact bridge columns, the load usually grows for a period of time due to the plastic deformation of the vehicle parts. However, the growth time is depended on the stiffness of vehicle [17]. Therefore, various shapes of triangular load with different growth time should be considered. Here, ζ is used to represent the ratio of load growth time to load duration time. When ζ is equal to 0.5, an isosceles triangle load shape is used, which is regarded to be a load shape of vehicle impact in some studies [18–21]. In Eurocode 1, it recommends that the shape of vehicle impact force is rectangular.

In summary, right triangle shape without time growth, triangle shape with time growth, and rectangle shape are the three types of loads used in the analysis of vehicle impact, as shown in Figure 2. In the paper, the effect of load shapes on the DAF of shear force is investigated in the following sections.

2.3. Improved Method for Structural Responses Calculation. The equation of motion based on the MTB theory proposed by Wan [16] is as follows:

$$\begin{cases} AG\mu\left(\dfrac{\partial y}{\partial x} - \varphi\right) = -EI\dfrac{\partial^2 \varphi}{\partial x^2} + \rho I\dfrac{\partial^3 y}{\partial x \partial t^2}, \\ AG\mu\left(\dfrac{\partial^2 y}{\partial x^2} - \dfrac{\partial \varphi}{\partial x}\right) + q = \rho A\dfrac{\partial^2 y}{\partial t^2}, \end{cases} \tag{2}$$

where φ is the cross section rotation caused by the bending deformation and μ is the shearing-shape coefficient of the cross section, which is used to modified the assumption that shear stress and shear strain are evenly distributed along the cross section, and the calculation methods can be referred to Hutchinson [22]. The term of $\rho I(\partial^3 y/\partial x \partial t^2)$ in equation (2) corresponds to the term of $\rho I(\partial^2 \varphi/\partial t^2)$ in the equation of motion of the CTB theory, which shows the difference between the CTB theory that only the rotational inertia caused by the bending deformation is considered and the MTB theory that rotational inertia caused by the shear deformation and the bending deformation are both considered.

To determine dynamic response using the mode superposition method of distributed mass systems, the first step is to calculate mode function $X_n(x)$, which is composed of transverse displacement function, $Y_n(x)$, and the angle of rotation of the cross section due to the bending moment, $\psi_n(x)$, of nth mode. In the second step, the generalized single degree of freedom equation is obtained based on mode orthogonality, and the modal amplitude, $T_n(t)$, is calculated by Duhamel integral. The corresponding response is calculated as follows:

$$r(x,t) = \sum_{n=1}^{\infty} X_n(x) T_n(t), \tag{3}$$

where $r(x,t)$ is the response referring to the internal force or deformation, which includes the first several modes contributing mostly to the responses.

During the process of the calculation of mode function based on the CTB theory, a critical frequency of ω_c (which is equal to $\sqrt{(AG\mu/\rho I)}$) exists since the rotational inertia caused by the shear deformation is ignored [15]. The solved natural frequency and modal functions have big errors compared to the actual value for ω larger than ω_c [16]. However, for the MTB theory, there is no cutoff frequency, and the mode function and natural frequency are more accurate [23]; the orthogonal conditions of the MTB theory are only applied for the symmetric boundary and symmetric loads. Therefore, to

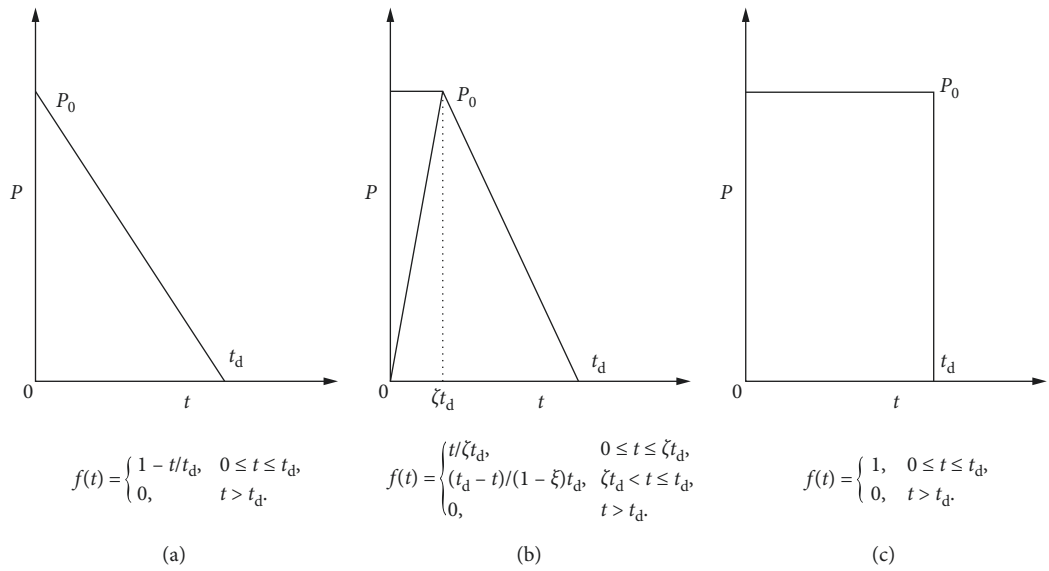

Figure 2: Different shapes of vehicle impact load. (a) Right triangle. (b) Triangle with time growth. (c) Rectangle.

accurately achieve the dynamic responses of bridge columns under impact load, an improved method is proposed (IMCTB) based on the MTB and CTB theories, and the calculation process is as follows.

2.3.1. Mode and Frequency Solution. For the nth mode, the displacement function, $Y_n(x)$, and bending angle function, $\psi_n(x)$, are assumed as follows:

$$\begin{cases} Y_n(x) = c_1 \cosh g_1 x + c_2 \sinh g_1 x + c_3 \cos g_2 x \\ \qquad + c_4 \sin g_2 x, \\ \psi_n(x) = c_1 g_3 \sinh g_1 x + c_2 g_3 \cosh g_1 x - c_3 g_4 \sin g_2 x \\ \qquad + c_4 g_4 \cos g_2 x, \end{cases} \tag{4}$$

where c_1, c_2, c_3, and c_4 are the normalized coefficients; g_1, g_2, g_3, and g_4 are the function of natural frequency of ω, which are calculated using following equation:

$$\begin{cases} g_{1,2} = \sqrt{\dfrac{\mp b^2\omega^2 + \sqrt{b^4\omega^4 + 4a^2\omega^2}}{2a^2}}, \\ g_3 = g_1\left(1 + \dfrac{\rho b^2\omega^2}{G\mu}\right) + \dfrac{EI}{AG\mu} g_1^3, \\ g_4 = g_2\left(1 + \dfrac{\rho b^2\omega^2}{G\mu}\right) + \dfrac{EI}{AG\mu} g_2^3, \\ a = \sqrt{\dfrac{EI}{\rho A}}, \\ b = \sqrt{\dfrac{I}{A}\left(1 + \dfrac{E}{G\mu}\right)}. \end{cases} \tag{5}$$

Based on the boundary condition listed in Table 1, the natural frequency of nth mode can be deduced combining with equation (2). Then, with natural frequency ω, and normalized coefficients c_1 through c_4, $Y_n(x)$, a, and $\psi_n(x)$ are obtained.

Table 1: Boundary conditions of bridge columns.

Boundary condition of bridge columns	Mathematical expressions
F-F	$Y(0) = Y(L) = 0; \psi(0) = \psi(L) = 0$
F-H	$Y(0) = Y(L) = 0; \psi(0) = 0; \psi\prime(L) = 0$

2.3.2. Amplitude Function Solution. The calculation of the amplitude function is based on the solution of natural frequency of ω and corresponding $Y_n(x)$ and $\psi_n(x)$.

It is assumed that the displacement and bending rotation of the column in y direction conform the following relationship:

$$\begin{cases} y(x,t) = \sum_{n=1}^{\infty} Y_n(x) T_n(t), \\ \varphi(x,t) = \sum_{n=1}^{\infty} \psi_n(x) T_n(t), \end{cases} \tag{6}$$

where $T_n(t)$ is the amplitude function of nth mode which shows the contribution to the response.

The orthogonal condition of the CTB theory is

$$\int_0^l \left(\rho A Y_n Y_m + \rho I \psi_n \psi_m\right) dx = 0, \tag{7}$$

Combining equations (6) and (7) and the motion equation of the CTB theory, the generalized differential equation for single degree of freedom is

$$\omega_n^2 T_n(t) M_n + \ddot{T}_n(t) Y_m = P_n(t), \tag{8}$$

where M_n and P_n are generalized mass and generalized load, which are given by

$$M_n = \int_0^l \left(\rho A Y_n^2 + \rho I \psi_n^2\right) dx. \tag{9}$$

For uniform distributed load,

$$P_n = \int_0^l q Y_n \, dx. \tag{10}$$

Employing Dirac integral to equation (10), the generalized load under concentrated impact load is

$$P_n = P_0 Y_n(\xi l) f(t). \tag{11}$$

With the solved mode functions of $Y_n(x)$ and $\psi_n(x)$, M_n and P_n are calculated, and the amplitude function of $T_n(t)$ is obtained with Duhamel integral employing to equation (8).

2.3.3. Internal Force Response. With the calculated mode functions of $Y_n(x)$, $\psi_n(x)$, and amplitude function of $T_n(t)$, the response under impact load based on the MTB is calculated. The shear force, Q, and bending moment, M, are as follows:

$$\begin{cases} Q = \sum_{n=1}^{\infty} AG\mu \left(Y_n' - \psi_n\right) T_n(t), \\ M = -\sum_{n=1}^{\infty} EI \psi_n' T_n(t). \end{cases} \tag{12}$$

3. Method Verification Using FEM

The time-history of shear force is calculated and analyzed based on the proposed method (IMCTB) and compared with the results from the CTB theory and FE analyses (using software ABAQUS) to validate the accuracy of IMCTB method. The information of the bridge columns with different slenderness ratios is shown in Table 2. The boundary condition of F-F is applied. The material density of ρ is 2500 kg/m^3, and modulus of elasticity of E is 30 GPa. The shape of impact load is right triangle without time growth, and the loading position is at midspan of the bridge column. The duration times are 0.015 s and 0.007 s to make the value of t_d/T_1 approximately equal to 1. The FE model adopts solid element of C3D8R with a mesh size of 0.02 m.

Firstly, the time-history curves of the shear force at the end section (SE), and the section that is about half cross section depth away from midspan (HD) of columns C06 and H14 are calculated as shown in Figure 1. Secondly, the peak value of the impact force (which is denoted as P_0) is applied as a static load at midspan and the static shear forces is obtained for each section. The time-history of dynamic amplification factor (DAF of shear force) is calculated as the ratio of the dynamic shear force to static shear force for the end section. The time-history within the fundamental period is analyzed.

Figure 3 shows the time-history curves of the DAF of shear force for columns C06 and H14. The results from the CTB theory, IMCTB method, and FE are presented and compared, where the first 100th order modes are taken using the CTB theory and IMCTB method. For C06, from Figures 3(a) and 3(b), the time-history curves of the DAF of shear force from the IMCTB method and the CTB theory are in good agreement with the ones from FE. At SE, the DAF of shear force reaches the maximum value of 2.64 at 0.0065 s. At HD, the shear transfer time was much shorter since it is close to the load position, and the shear forces increases initially. The DAF of shear force reaches the maximum value of 1.43 at 0.005 s.

For Column H14 as shown in Figures 3(c) and 3(d), the results show good agreements with those from FE, but the results using the CTB theory show large differences. As shown in Figure 3(c), at 0.0038 s, the maximum DAF of shear force using the CTB theory reaches 3.58, which is larger than that from FE (2.75), and the maximum DAF of shear force from the IMCTB method is 2.77, which is close to FE. Moreover, as shown in Figure 3(d), the maximum DAF of shear force using the CTB theory is 2.70 at 2.8 ms, which is significantly larger than the results from FE analysis (1.65) and the IMCTB method (1.67).

The critical frequency in the CTB theory for columns C06 and H14 occurs at 12th and 4th modes, respectively. The dynamic internal force response is mainly influenced by the first several modes, which means the CTB theory can produce large errors especially when the slenderness ratio is smaller. However, it indicates that the DAF of shear force calculation using the IMCTB method shows good agreements with FE analysis results, especially for the columns with small slenderness ratios.

4. Characteristics of DAF of Shear Forces under Impact Load

More accurate solution of elastic internal forces of bridge columns at any section at any time can be obtained using the proposed method (IMCTB) in this paper. The ratio between the dynamic internal force at a certain moment and the static internal force at SE is the distribution of DAF along the column height. Figures 4(a) and 4(b) gives the DAF distributions of shear force and bending moment in C10 at 0.5 ms and 5 ms for a load shape of right triangle with t_d/T_1 of 1.

At 0.5 ms, the shear force and bending moment mostly distribute within a range from 1 m to 4 m away from the column end, which indicates that the bridge column effective length is shorter than the actual length and the shear failure easily occurs under this circumstance due to the effect of inertia force. Therefore, the failure mode of column may transform from bending failure under static load to shear failure under impact load.

If the column does not fail at the initial stage (0.5 ms), the DAF distributions of the elastic internal forces at 5 ms are presented in Figure 4(b). Figure 4(b) shows the values of DAF are larger than those at 1 ms. The DAFs of shear force and bending moment at midspan of the column are around 0.5 and 1.0, respectively. The DAF of shear force is greater than 1.5 within the range from 0 m to 1.5 m away from SE section and approaches 2.0 at SE, while the DAF of the bending moment is around 1.5 at SE section. Therefore, if the strength of column can withstand the internal force generated by the early-stage dynamic response, then at this

Table 2: Parameters of bridge columns.

No.	Length (m)	Height/diameter (m)	Width (m)	Slenderness ratio	Fundamental period T_1 (s)	Duration time, t_d (s)	t_d/T_1
C06	5	0.6	—	16.7	0.0146	0.015	1.03
H14	5	1.4	0.5	6.19	0.0072	0.007	0.97
C10	5	1.0	—	10	0.0096	0.010	1.04

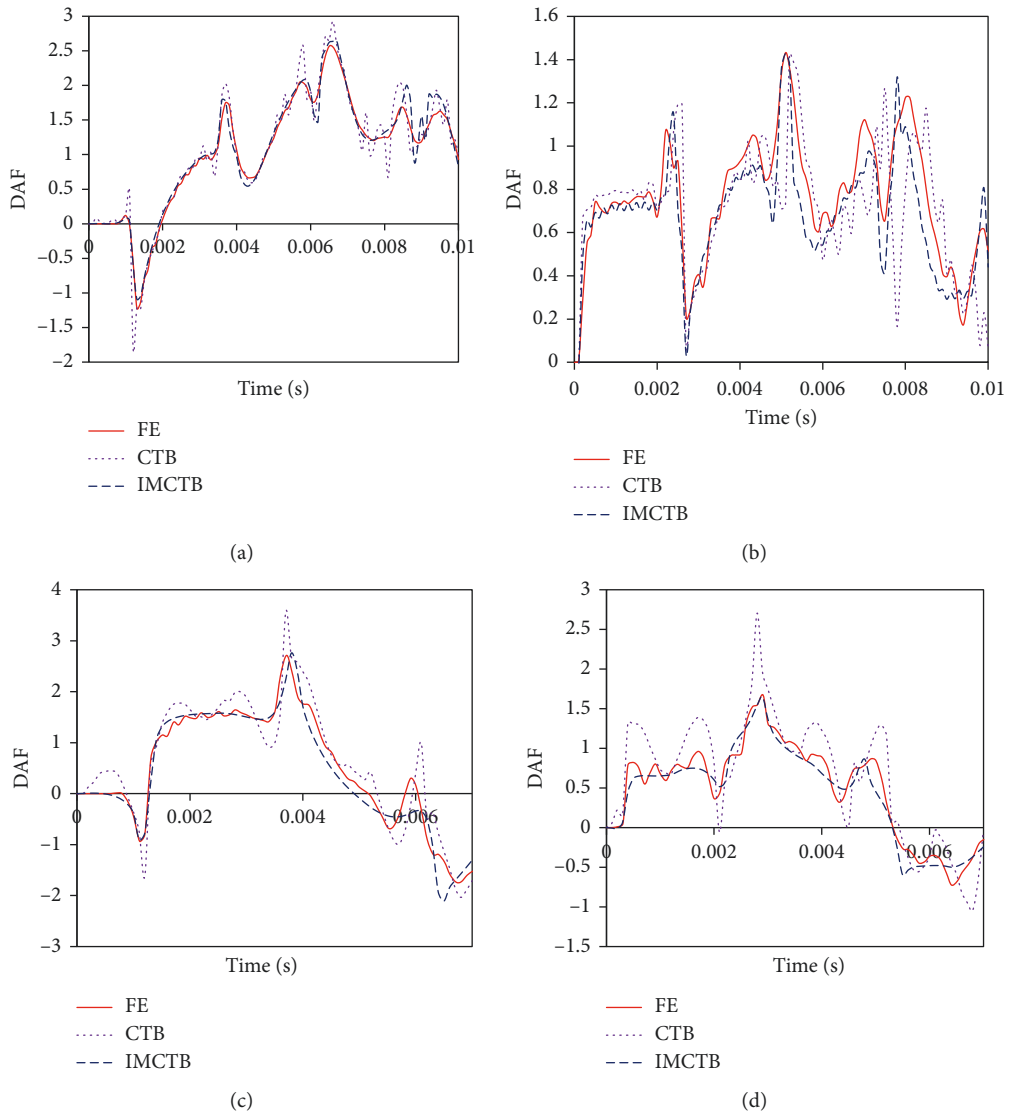

Figure 3: The time-history curves of DAF of shear forces for columns under impact load. (a) Shear force time-history of C06 at SE. (b) Shear force time-history of C06 at HD. (c) Shear force time-history of H14 at SE. (d) Shear force time-history of H14 at HD.

moment, flexural shear failure or shear failure may occur at the end of column due to insufficient strength.

Figure 4(c) presents the DAF distributions of the internal forces in C10 at 20 ms for a load shape of right triangle with t_d/T_1 of 4. The results show that the distributions of the internal forces are the same as those under static load. Therefore, for the impact load with long growth time and large t_d/T_1, the dynamic response within the bridge column can be ignored and the impact load can be treated as a static load.

In summary, the calculated shear forces of bridge columns under impact load using IMCTB is more practical and accurate than the ones using the CTB theory, especially for the columns with small slenderness ratio. In addition, the calculated distribution of elastic internal forces of bridge columns at various times can be utilized to analyze the causes of different failure modes. As shown in Figures 3 and 4, the maximum DAF of shear force occurs at the end section, which can be used as the DAF of shear forces for bridge columns under impact load.

5. Parametric Studies on DAF of Shear Force

As the analyses above, the dynamic effect of bridge columns under impact load is related to many factors such as load

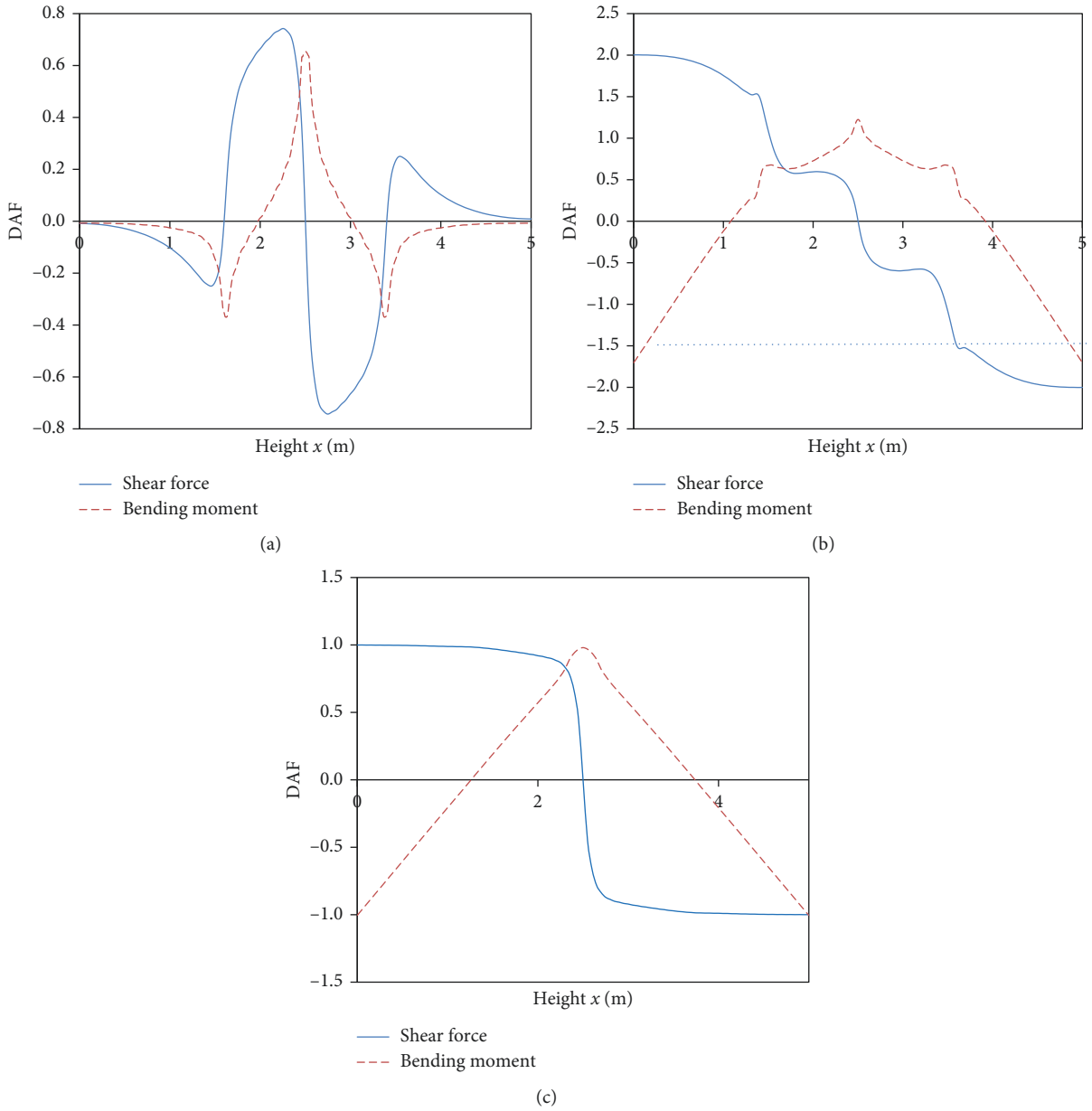

FIGURE 4: Distribution of DAF of internal forces of bridge columns at different timestamps under impact load. (a) Right triangle of $t_d/T_1 = 1$, 0.5 ms. (b) Right triangle of $t_d/T_1 = 1$, 5 ms. (c) Isosceles triangle of $t_d/T_1 = 4$, 20 ms.

characteristics, boundary condition, slenderness ratio, and load position, which are investigated in this section. As described in Section 3, the maximum DAF of shear force at section SE is larger than that at section HD; as described in Section 4, the maximum shear force at section SE is larger than that at the other section. Therefore, the maximum DAF of shear force (DAF (max)) at section SE is used to represent the dynamic effect of bridge column. Four factors are included in this paper.

In a curve plot of DAF (max), x-axis is the ratio of load duration (t_d) to natural period (T_1), and y-axis is the DAF (max).

(1) Load characteristics, including load shape and duration time. Since there is no generally accepted shape for vehicle impact force, three shapes of impact load in Section 2.3 are investigated. For the shape of triangular load pulse with growth time, ζ with a value of smaller or equal to 0.5 is taken.

(2) Boundary conditions. Two boundary conditions of F-F and F-H shown in Section 2.2 are analyzed [24].

(3) Slenderness ratio. The values of 6 to 20 and 8 to 28 are used for F-F and F-H conditions, respectively, based on the research and accidents statistics [2, 25–27].

(4) Load position. In this paper, a distance from the column end is used in the paper. ξ is used to denote the ratio of this distance to the column height varying between 0.1 and 0.5.

5.1. Load Shape of Right Triangle

5.1.1. Slenderness Ratio. Figure 5 gives the maximum DAF (DAF (max)) of shear force of bridge columns under impact load with a shape of right triangle without growth time for F-F and F-H boundary conditions. It is found the DAF (max) of shear force increases with t_d/T_1 increase. The DAF (max) increases rapidly when t_d/T_1 smaller than 5 but gradually approaches an asymptotic value after, while the DAF (max) of shear force does not show a monotonic trend with the increase of slenderness ratio. With the comparison of the DAF (max) for F-F and F-H boundary conditions, it is found that the slenderness ratio has more significant effect on F-F column than F-H column. The DAF (max) for F-H column is smaller than that for F-F column. For instance, the DAF (max) for F-F column with slenderness ratio of 8.3 and F-H column with slenderness ratio of 11.6 (same cross section) are 4.2 and 2.79, respectively, when t_d/T_1 is equal to 10. The results of the DAF (max) are significantly larger than the upper bound of 2.0 for the DAF (max) derived using the SDOF method.

5.1.2. Load Position. Figure 6 gives the maximum DAF of shear for bridge columns under right triangle impact load applied on different positions. It shows that the closer the load position is to the end, the smaller the DAF (max) of shear force is, which indicates the dynamic effect is lower when the load position is near to the end of the columns. For example, when ξ equals to 0.1, the DAF (max) of FF column approaches 2 with the increase of t_d/T_1; when ξ equals to 0.3, the DAF (max) of FF column approaches 2.58 with the increase of t_d/T_1; and when ξ equals to 0.5, the DAF (max) of FF column approaches 4.24 with the increase of t_d/T_1. The maximum dynamic response occurs when the load acts on the midspan position.

5.2. Load Shape of Triangle with Time Growth

5.2.1. Slope of Load Growth. Figure 7 presents the DAF (max) curves of shear force for bridge columns when subjected to impact load at midspan with different slopes of load growth, where F-F column and F-H column with slenderness ratios of 10 and 14, respectively, are investigated. It shows the DAF (max) of shear force increases gradually with t_d/T_1 increase when ζ equal to 0.01, and gradually approaches to a certain value, which is similar to the results of the column under impact load of right triangle in Section 5.1. When ζ is larger than 0.01, the DAF (max) of shear force increases gradually to the maximum with t_d/T_1 increase, and then decreases. For larger value of ζ, the decrease occurs earlier; When ζ is larger than 0.1 and t_d/T_1 is larger than 4, the DAF (max) of shear force is close to 1, which can be treated as quasi-static loading; the DAF (max) of shear force can be reduced with the increase of ζ when t_d/T_1 stays the same.

It is an isosceles triangle load when ξ equals to 0.5, and it is regarded as the shape of vehicle impact load by Thilakarathna et al. [18–21]. As shown in Figure 7, it is found that when the column is subjected to impact load at midspan, the DAF (max) of shear force increases firstly with t_d/T_1 increase and approaches the maximum when t_d/T_1 is around 1.0, and then decreases. The DAF (max) of shear force of F-F column is approximately 1.9, which is increased about 27% compared with the results of 1.5 from the SDOF method. Additionally, the isosceles triangle load can be treated as a quasi-static load when t_d/T_1 larger than 4, and the value of DAF (max) can be taken as 1.0.

5.2.2. Slenderness Ratio. Figure 8 shows the DAF (max) curves of shear forces for bridge columns with different slenderness ratios subjected to triangle impact load with different growth time. The results show the curves of DAF (max) with different slenderness ratios are very close when ζ equals to 0.05; when ζ equals to 0.5, the curves of DAF (max) have been overlapped, which indicates the slenderness ratio has little effect. Thus, for ζ equal to or larger than 0.05, the effect of slenderness ratio can be ignored.

5.2.3. Load Position. Figure 9 gives the maximum DAF of shear force under impact load with isosceles triangle shape at different load positions. The results show that DAF (max) decreases when the load position gets closer to the end; when ξ equals to 0.1, the curve of DAF (max) approaches a horizontal line approximately with a constant value of 1.1. Thus, the DAF (max) of shear force is generated when the load position is at midspan of the column.

5.3. Load Shape of Rectangle

5.3.1. Slenderness Ratio. Figure 10 shows the maximum DAF of shear forces for F-F and F-H columns under rectangle impact load at midspan with different slenderness ratios. When t_d/T_1 is larger than 0.5, the DAF (max) of shear force becomes stable with a constant value. It is found the DAF (max) of F-F column is significantly influenced by slenderness ratio, but it does not change monotonously with slenderness ratio increase. However, the DAF (max) of F-H column is less influenced by slenderness ratio, and the values are stable with a value between 2.7 and 3.0 when t_d/T_1 is larger than 0.5. All the results are significantly higher than the value of 2.0 calculated from the SDOF method.

5.3.2. Load Position. Figure 11 gives the maximum DAF of shear force under rectangle impact load at different positions for F-F column with slenderness ratio of 10, and F-H column with slenderness ratio of 14. Similarly, the DAF (max) decreases when the load position is closer to the end, which highlights the maximum DAF of shear force occurs when the load position is at midspan of columns.

6. Simplified Formula of DAF of Shear Force

6.1. Simplified Formula. With the parametric studies in Section 5, it shows that different factors can have different effects on the DAF (max) of shear force, and it is difficult

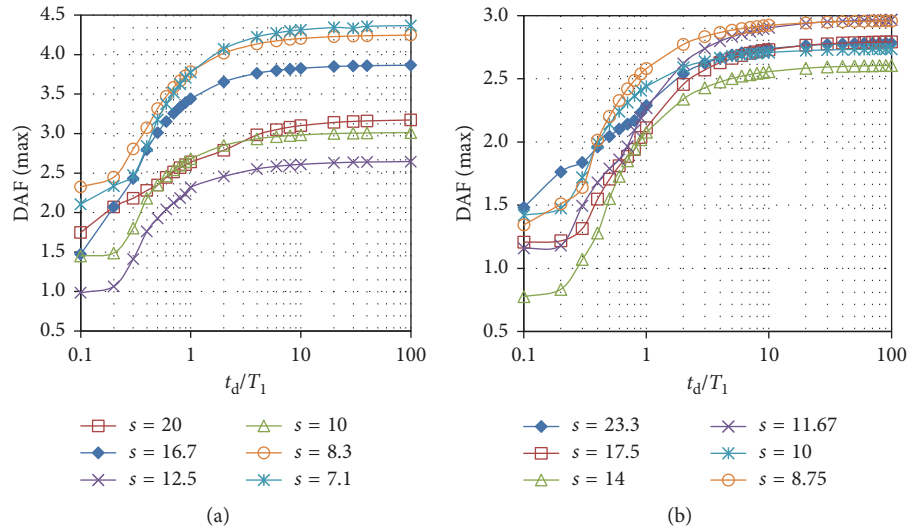

Figure 5: DAF (max) of shear force of bridge columns under impact load with right triangle shape for different boundary conditions. (a) F-F. (b) F-H.

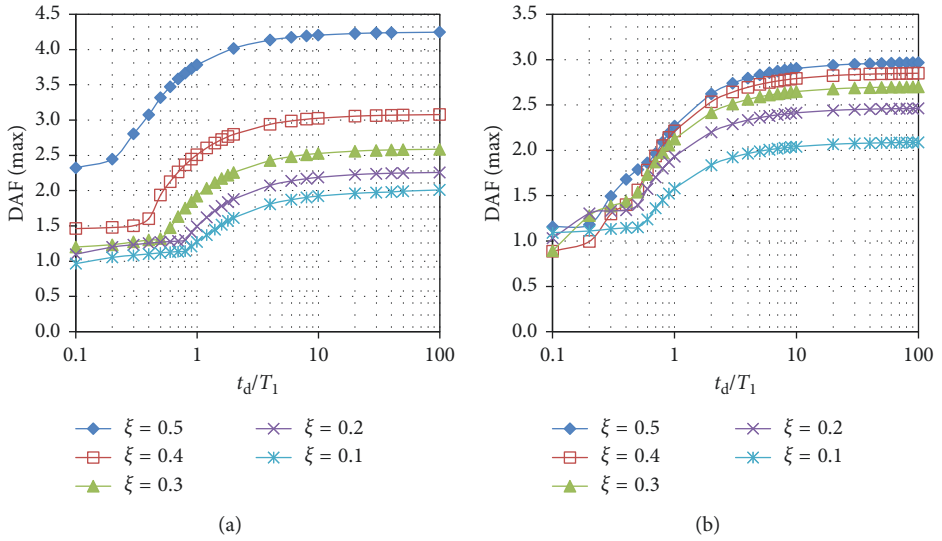

Figure 6: DAF (max) of shear force of bridge columns under impact load applied to different positions with right triangle shape. (a) F-F. (b) F-H.

to determine DAF (max) for various conditions with consideration of all the factors. In this section, the data of DAF (max) of shear force based on the parametric studies are regressed to form approximate formula. As analyzed in Section 4, the results of DAF (max) curves under various load shapes vary significantly; therefore, different formula should be applied. Moreover, it is found the results of DAF (max) of shear force for F-H column is slightly lower than that for F-F column; therefore, only the DAF (max) of shear force for F-F column is considered conservatively.

6.1.1. Load Shape of Right Triangle without Time Growth. It is shown in Figure 5 that the DAF (max) curves are consistent with the shape of growth model, thus growth model is used to regress and fit, and the formula for the maximum DAF of shear force is proposed as follows:

$$\mathrm{DAF\,(max)} = \frac{\beta_2}{1 + [(\beta_2 - \beta_0)/\beta_0]e^{\beta_1 t_d/T_1}}, \tag{13}$$

where $\beta_0, \beta_1, \beta_2$ are calculated as follows:

$$\begin{cases} \beta_0 = 1.635 - 0.097s - 3.936\xi + 0.004s^2 + 7.086\xi^2 + 0.073s\xi, \\ \beta_1 = -1.844, \\ \beta_2 = 2.962 - 0.129s - 3.144\xi + 0.004s^2 + 7.824\xi^2 + 0.132s\xi, \end{cases} \tag{14}$$

where s is the slenderness ratio of a bridge column.

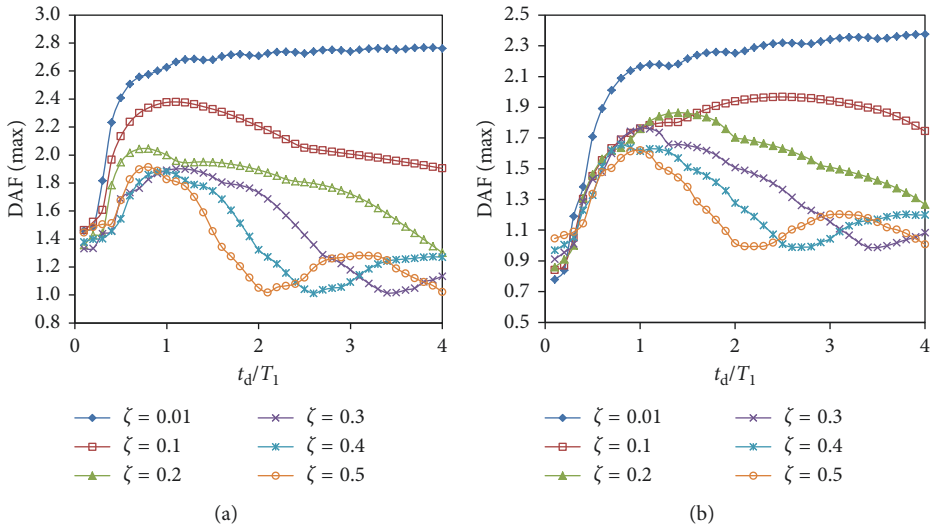

Figure 7: DAF (max) curves of shear force of bridge columns under impact load at midspan with different slopes of load growth. (a) F-F. (b) F-H.

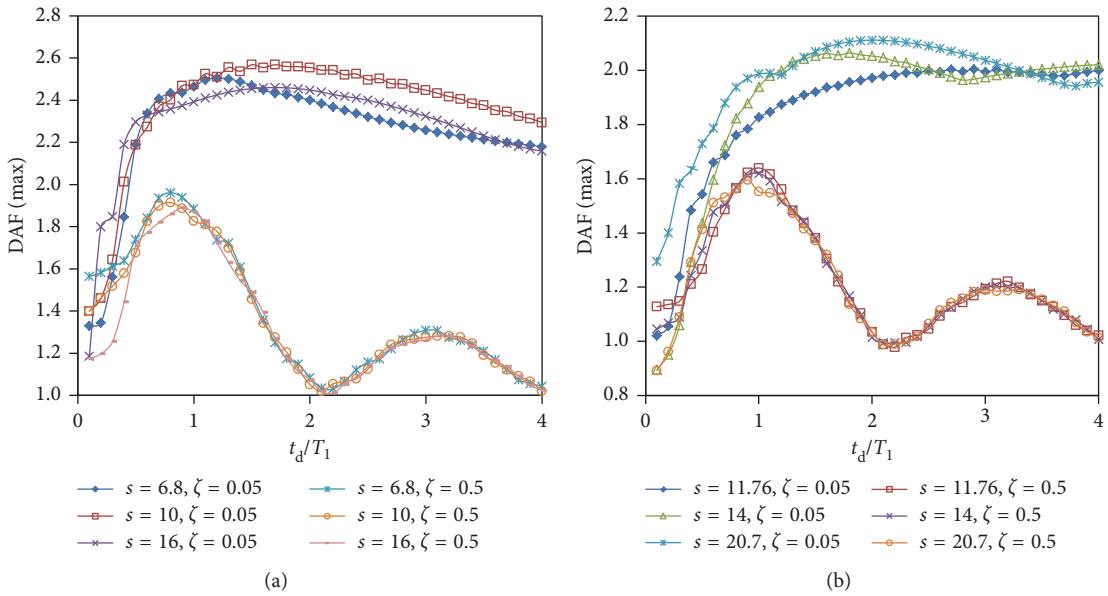

Figure 8: Maximum DAF of shear forces of bridge columns with different slenderness ratios under impact load with triangle shape and growth time. (a) F-F. (b) F-H.

6.1.2. Load Shape of Triangle with Time Growth. Load shape of isosceles triangle is widely used as the form of vehicle impact load; therefore, only ζ equal to 0.5 is considered. The slenderness ratio has little effect on the maximum DAF of shear force (Section 5) and is ignored here. The regressed formulation is

$$\begin{aligned}\mathrm{DAF(max)} = {} & 1.022 + 0.12t_1 - 0.22t_1^2 + 0.048t_1^3 \\ & + 0.414\xi - 5\xi^2 + 12.143\xi^3 + 1.776\xi t_1 \\ & - 2.19\xi^2 t_1 - 0.22\xi t_1^2,\end{aligned} \quad (15)$$

where t_1 equals to t_d/T_1 with a value of smaller than 4, and the impact load can be regarded as a static load when t_d/T_1 larger than 4.

6.1.3. Load Shape of Rectangle. Generally, the duration time of impact load is 0.5 times greater than that of the first-order natural vibration period of bridge columns. Therefore, the conditions of t_d/T_1 larger than 0.5 is only considered for rectangle load shape, and the regressed formulation is

$$\mathrm{DAF(max)} = 7.73 + 0.146s'^4 - 1.963s'^3 + 7.63s'^2 - 10.557s', \quad (16)$$

where s' is equal to $s/10$ within a value ranging from 0.6 to 2.

6.2. Case Study. A concrete bridge column with diameter of 1 m and height of 5 m is used as the studied case. The column is fixed at both ends with a slenderness ratio of 10. The

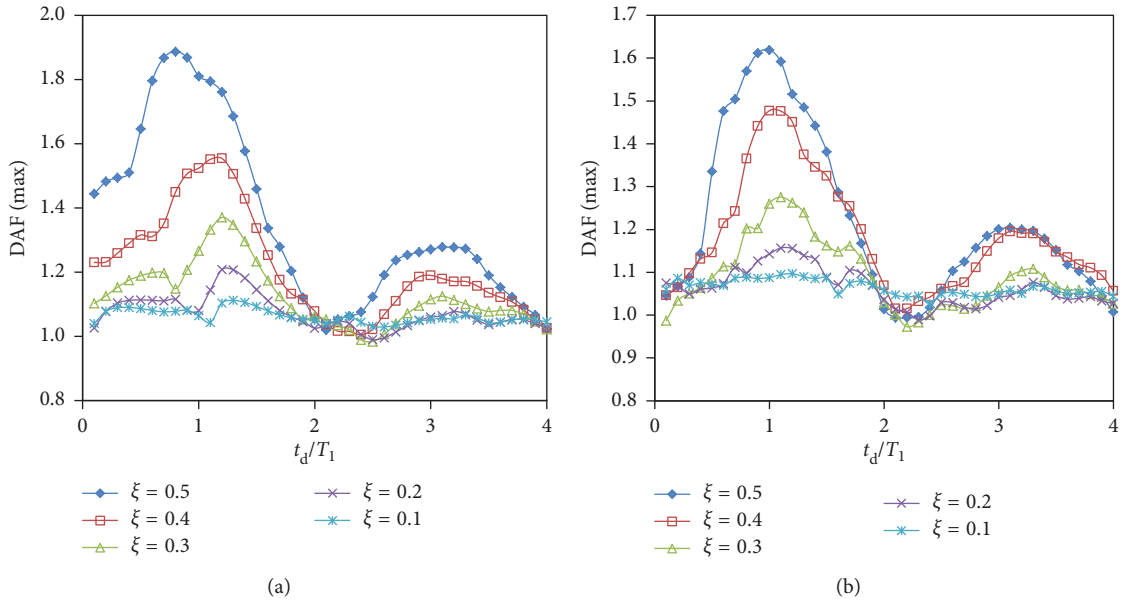

Figure 9: Maximum DAF of shear force of bridge columns under impact load with isosceles triangle shape at different positions. (a) F-F. (b) F-H.

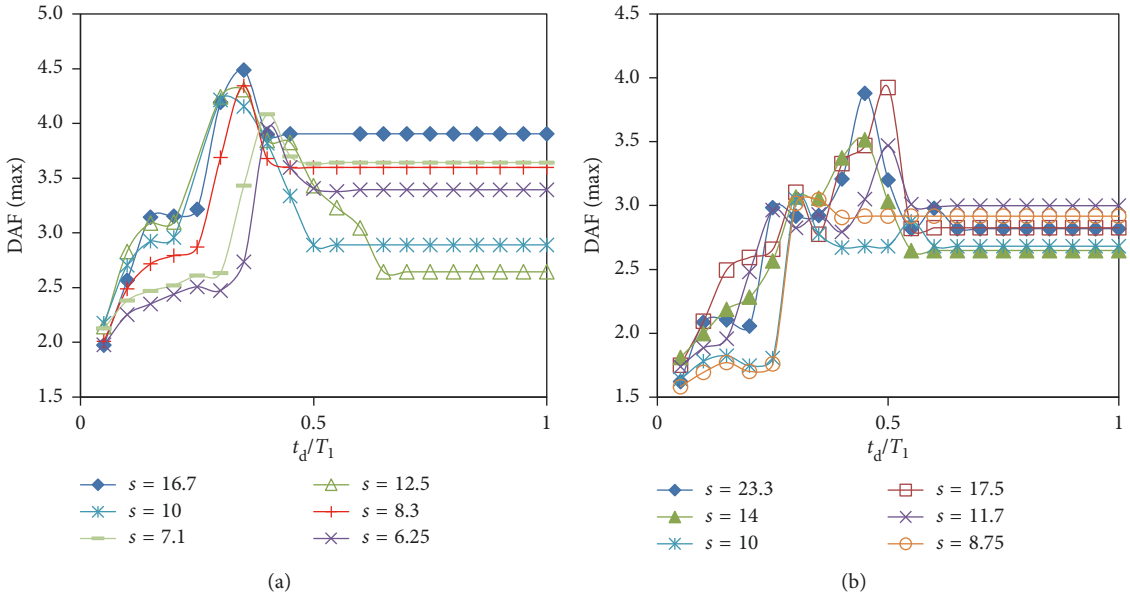

Figure 10: Maximum DAF of shear force of bridge columns with different slenderness ratios subjected to rectangle load pulse. (a) F-F. (b) F-H.

density and elastic modulus of the concrete are 2500 kg/m^3 and 30 GPa, respectively. The first-order natural vibration period of T_1 is 9.6 ms.

Firstly, the proposed simplified formula is verified using FE analysis. It was estimated that the impact force of a 30 t vehicle collision at 64 km/h can be divided into two parts: (a) a short-time load with a peak value of 7500 kN and duration time of 10 ms when the engine or gearbox hits the column and (b) a long-time load with a peak value of 5800 kN and duration time of 90 ms when rear part of the vehicle hits the column [28]. Therefore, the loading duration of 10 ms and 90 ms are both studied. The t_d/T_1 for short-time and long-time loads are 1 and 10, respectively. Moreover, the load shapes of right triangle, isosceles triangle, and rectangle are considered, and the load position is at a distance of 1.5 m away from the column end. Table 3 gives the calculated maximum DAF of shear force at the column end based on the proposed simplified formula and FE analysis, and the results show that the proposed simplified formulas have high accuracy.

In Annex C of Eurocode 1: Part 1–7, the impact force of a vehicle with a mass of 30 t and a speed of 90 km/h is 2400 kN, and the specification gives a DAF (max) of 1.4. The load duration of 10 ms and 90 ms, and the load shape of right

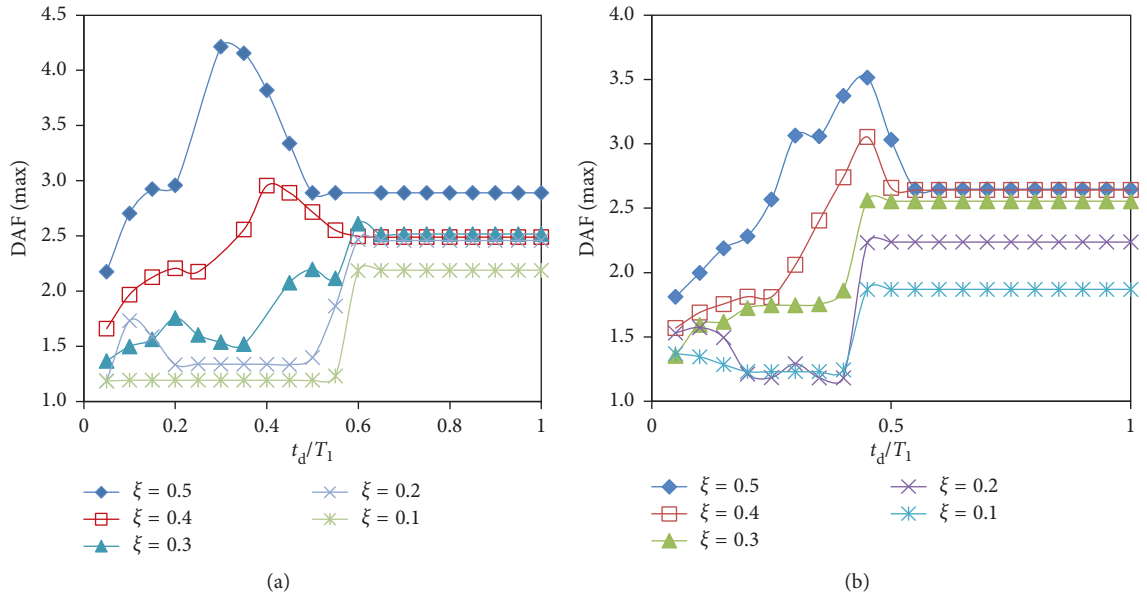

Figure 11: Maximum DAF of shear force of bridge columns under rectangle impact load at different positions. (a) F-F. (b) F-H.

Table 3: The calculated DAFs of shear force based on proposed practical formula.

Method	Right triangle		Isosceles triangle		Rectangle	
	$t_d/T_1 = 1$	$t_d/T_1 = 10$	$t_d/T_1 = 1$	$t_d/T_1 = 10$	$t_d/T_1 = 1$	$t_d/T_1 = 10$
IMCTB	1.69	2.23	1.26	1.0	2.25	2.25
FE	1.69	2.17	1.27	1.0	2.22	2.15

triangle, isosceles triangle, and rectangular were considered. The static force of 2400 kN is applied at the height of 1.5 m from the bottom of the column to obtain the shear force at the section of the column end. Then, the shear force is multiplied by the DAF (max) to obtain the shear demand. The maximum shear forces of column end calculated from the proposed simplified formulas and the current design codes are given in Table 4. The shear demand obtained from AASHTO-LRFD (2012) is also shown in the table. The maximum dynamic shear forces from the proposed method are larger than that from the current design codes, and the forces are depended on the load shape and duration time of the impact load. Therefore, the current design codes may be insufficient to estimate the shear demands of bridge columns under impact load. Except the DAF (max) of shear force, future study needs for the load shape, peak value, and duration of impact load that often occurs for bridge columns.

Table 4: Shear demands of bridge columns under impact load based on different calculation methods.

Calculation method	Calculation condition	Shear demand (kN)
Specifications	AASHTO-LRFD	2093
	EN 1991-1-7 Table C.2	2633
Proposed method (IMCTB)	Right triangle, $t_d/T_1 = 1$	3180
	Right triangle, $t_d/T_1 = 10$	4195
	Isosceles triangle, $t_d/T_1 = 1$	2370
	Isosceles triangle, $t_d/T_1 = 10$	1881
	Rectangle, $t_d/T_1 = 1$	4237
	Rectangle, $t_d/T_1 = 10$	4237
	Rectangle, $t_d/T_1 = 32.3$	4237

7. Conclusions

This paper proposes a novel method (IMCTB) to determine the dynamic load effects of bridge columns under different boundary conditions and different load positions subject to concentrated impact load, and parametric studies on the DAF of shear force are conducted. Additionally, the simplified formula are regressed and verified with a case study. Major findings are summarized as follows:

(1) For bridge columns with small slenderness ratios, the dynamic responses calculated using IMCTB under impact load are more practical and accurate than that using the CTB theory under concentrated impact load.

(2) The characteristics of impact load can cause different dynamic response of bridge columns, which can affect the failure modes. For the impact load with long growth time and large t_d/T_1, the dynamic response can be ignored, and the impact load can be treated as a static load applied to the bridge columns.

(3) The maximum DAF of shear force of bridge columns under load shape of right triangle without time growth and load shape of rectangle is relevant to slenderness ratio. For a column with a certain slenderness ratio subjected to right triangle impact load, the maximum DAF of shear force increases

with the ratio of load duration time to first-order natural vibration period, t_d/T_1, and then approaches an asymptotic value.

(4) For load shape of triangle with time growth, the larger the ratio of load growth time to load duration time is, the smaller of the maximum DAF of shear force is obtained. For load shape of isosceles triangle, the maximum DAF of shear force approaches the maximum when t_d/T_1 is about 1.0. For load shape of rectangle, the maximum DAF of shear force is a constant when t_d/T_1 is larger than 5.0.

(5) The closer the load position is to the end, the smaller the maximum DAF of shear force is, indicating that the maximum DAF of shear force occurs when the load position is at midspan of bridge columns. Moreover, the maximum DAF of shear force for bridge columns with both ends fixed is larger than that with bottom fixed and top hinged. Therefore, the boundary condition with both ends fixed can be conservatively considered.

(6) The proposed regressed formula in this paper is simple and precise to calculate the maximum DAF of shear force under different conditions with different parameters. The case study shows that the current design codes underestimate the shear demand of bridge columns under impact load; a further study on vehicle impact for bridge columns is necessary.

Data Availability

The data used to support the findings of this study are included within the article.

Conflicts of Interest

The authors declare that there are no conflicts of interest regarding the publication of this paper.

Acknowledgments

Research funding provided by the National Natural Science Foundation of China (Grant nos. 51438010 and 51608378) and Science and Technology Commission of Shanghai Municipality (18DZ1201203 and 17DZ1204300) is gratefully acknowledged.

References

[1] L. Chen and Y. Xiao, "Review of studies on vehicle anti-collision on bridge piers," *Journal of Highway and Transportation Research and Development*, vol. 29, no. 8, pp. 78–86, 2012.

[2] E. C. Buth, W. F. Williams, M. S. Brackin, D. Lord, S. R. Geedipally, and A. Y. Abu-Odeh, *Analysis of Large Truck Collision with Bridge Piers-Report of Guidelines for Designing Bridge Piers and Abutments for Vehicle Collisions 9-4973-1*, Texas Transportation Institute, The Texas A&M University, College Station, TX, USA, 2009.

[3] E. B. Williamson, *Blast-Resistant Highway Bridges-Design and Detailing Guidelines*, Transportation Research Board, Washington DC, USA, 2010.

[4] S. Saatci and F. J. Vecchio, "Effects of shear mechanisms on impact behavior of reinforced concrete beams," *ACI Structural Journal*, vol. 106, no. 1, pp. 78–86, 2009.

[5] S. D. Adhikary, B. Li, and K. Fujikake, "Low velocity impact response of reinforced concrete beams: experimental and numerical investigation," *International Journal of Protective Structures*, vol. 6, no. 1, pp. 81–111, 2015.

[6] American Association of State Highway and Transportation Officials (AASHTO), *AASHTO LRFD Bridge Design Specifications*, American Association of State Highway and Transportation Officials, Washington, DC, USA, 2012.

[7] C. E. Buth, M. S. Brackin, W. F. Williams, and G. T. Fry, *Collision Loads on Bridge Piers: Phase 2, Report of Guidelines for Designing Bridge Piers and Abutments for Vehicle Collisions*, No. FHWA/TX-11/9-4973-2, Texas Transportation Institute, The Texas A&M University, College Station, TX, USA, 2011.

[8] European Committee For Standardization, *BS EN 1991-1-7: 2006: Eurocode 1: Actions on Structures-Part 1–7: General Actions-Accidental Actions*, European Committee For Standardization, London, UK, 2010.

[9] J. M. Biggs and B. Testa, *Introduction to Structural Dynamics*, McGraw-Hill, Vol. 3, McGraw-Hill, New York, NY, USA, 1964.

[10] Q. Qian and M. Y. Wang, *Calculation Theory for Advanced Protective Structures*, Phoenix Publishing and Media Group, Nanjing, China, 2009, in Chinese.

[11] S. El-Tawil, E. Severino, and P. Fonseca, "Vehicle collision with bridge piers," *Journal of Bridge Engineering*, vol. 10, no. 3, pp. 345–353, 2005.

[12] J. Magnusson, M. Hallgren, and A. Ansell, "Shear in concrete structures subjected to dynamic loads," *Structural Concrete*, vol. 15, no. 1, pp. 55–65, 2014.

[13] Q. Fang, D. Guo, Y. D. Zhang, and J. C. Liu, "Determination of shear dynamic factor in beams," *Engineering Mechanics*, vol. 22, no. 5, pp. 181–185, 2005, in Chinese.

[14] N. Jones, *Structural Impact*, Cambridge University Press, Cambridge, UK, 2011.

[15] S. M. Han, H. Benaroya, and T. Wei, "Dynamics of transversely vibrating beams using four engineering theories," *Journal of Sound and Vibration*, vol. 225, no. 5, pp. 935–988, 1999.

[16] C. F. Wan, "Modification of motion equation of Timoshenko beam and its application in structural impact response," Master thesis, Tongji University, Shanghai, China, 2003, in Chinese.

[17] H. Al-Thairy and Y. C. Wang, "Simplified FE vehicle model for assessing the vulnerability of axially compressed steel columns against vehicle frontal impact," *Journal of Constructional Steel Research*, vol. 102, pp. 190–203, 2014.

[18] H. M. I. Thilakarathna, D. P. Thambiratnam, M. Dhanasekar, and N. Perera, "Numerical simulation of axially loaded concrete columns under transverse impact and vulnerability assessment," *International Journal of Impact Engineering*, vol. 37, no. 11, pp. 1100–1112, 2010.

[19] I. Thilakarathna, D. Thambiratnam, M. Dhanasekar, and N. Perera, "Shear-critical impact response of biaxially loaded reinforced concrete circular columns," *ACI Structural Journal*, vol. 110, no. 4, pp. 565–574, 2013.

[20] H. Thilakarathna, D. Thambiratnam, M. Dhanasekar, and N. Perera, "Infrastructure sustainability: vulnerability of axially

loaded columns subjected to transverse impact loads," in *Rethinking Sustainable Development Urban Management Engineering & Design*, IGI Global, Hershey, PA, USA, 2010.

[21] H. Thilakarathna and I. Mudiyanselage, *Vulnerability assessment of reinforced concrete columns subjected to vehicular impacts*, Ph.D. thesis, Queensland University of Technology, Brisbane, Australia, 2010.

[22] J. R. Hutchinson, "Shear coefficients for Timoshenko beam theory," *Journal of Applied Mechanics*, vol. 68, no. 1, pp. 87–92, 2001.

[23] D. Y. Bian, "Defect of Timoshenko beam theory and correction of motion equation," Master thesis, Tongji University, Shanghai, China, 2008, in Chinese.

[24] G. D. Williams and E. B. Williamson, "Response of reinforced concrete bridge columns subjected to blast loads," *Journal of Structural Engineering*, vol. 137, no. 9, pp. 903–913, 2011.

[25] Y. Xia, H. Nassif, and D. Su, "Early-age cracking in high performance concrete decks of a curved steel girder bridge," *Journal of Aerospace Engineering*, vol. 30, no. 2, article B4016003, 2017.

[26] X. Shi, Z. Cao, H. Ma, and X. Ruan, "Failure analysis on a curved girder bridge collapse under eccentric heavy vehicles using explicit finite element method: case study," *Journal of Bridge Engineering*, vol. 23, no. 3, article 05018001, 2018.

[27] S. El-Tawil, *Vehicle Collision with Bridge Piers, FDOT CONTRACT BC-355-6*, University of Michigan, Ann Arbor, MI, USA, 2004.

[28] A. Ghose, "Strategies for the management of bridges for vehicular impacts," *Proceedings of the Institution of Civil Engineers-Structures and Buildings*, vol. 162, no. 1, pp. 3–10, 2009.